iScience

CellPress
OPEN ACCESS

Article

Canonical Wnt signaling induces focal adhesion and Integrin beta-1 endocytosis

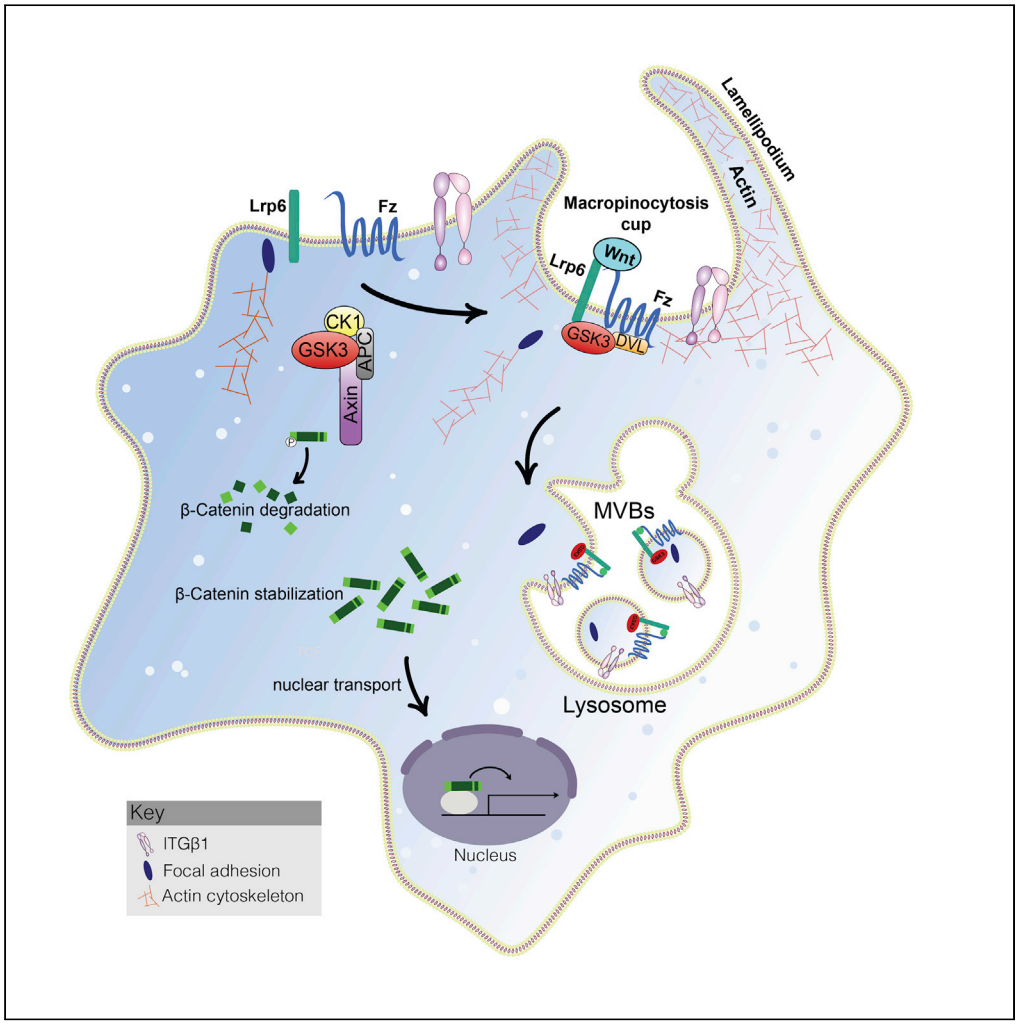

Nydia Tejeda-Muñoz, Marco Morselli, Yuki Moriyama, Pooja Sheladiya, Matteo Pellegrini, Edward M. De Robertis

ntejedamunoz@mednet.ucla.edu (N.T.-M.)
ederobertis@mednet.ucla.edu (E.M.D.R.)

Highlights

Wnt protein treatment triggers rapid endocytosis of focal adhesion components

Integrin-β1 is depleted form the cell surface by Wnt within minutes

In *Xenopus* assays, Integrin-β1 depletion inhibits Wnt overexpression

The canonical Wnt and focal adhesion signaling pathways crosstalk via endocytosis

Tejeda-Muñoz et al., iScience *25*, 104123
April 15, 2022
https://doi.org/10.1016/j.isci.2022.104123

iScience

CellPress
OPEN ACCESS

Article

Canonical Wnt signaling induces focal adhesion and Integrin beta-1 endocytosis

Nydia Tejeda-Muñoz,[1,*] Marco Morselli,[2] Yuki Moriyama,[1,3] Pooja Sheladiya,[1] Matteo Pellegrini,[4] and Edward M. De Robertis[1,5,*]

SUMMARY

During canonical Wnt signaling, the Wnt receptor complex is sequestered together with glycogen synthase kinase 3 (GSK3) and Axin inside late endosomes, known as multivesicular bodies (MVBs). Here, we present experiments showing that Wnt causes the endocytosis of focal adhesion (FA) proteins and depletion of Integrin β 1 (ITGβ1) from the cell surface. FAs and integrins link the cytoskeleton to the extracellular matrix. Wnt-induced endocytosis caused ITGβ1 depletion from the plasma membrane and was accompanied by striking changes in the actin cytoskeleton. *In situ* protease protection assays in cultured cells showed that ITGβ1 was sequestered within membrane-bounded organelles that corresponded to Wnt-induced MVBs containing GSK3 and FA-associated proteins. An *in vivo* model using *Xenopus* embryos dorsalized by *Wnt8* mRNA showed that ITGβ1 depletion decreased Wnt signaling. The finding of a crosstalk between two major signaling pathways, canonical Wnt and focal adhesions, should be relevant to human cancer and cell biology

INTRODUCTION

Recent work has shown a fundamental role for membrane trafficking in the cell biology of canonical Wnt signaling (Albrecht et al., 2021) in addition to the well-established transcriptional effects mediated by β-catenin stabilization (Nusse and Clevers, 2017). Binding of the Wnt growth factors to the Frizzled (Fz) and LDL-receptor related protein 6 (LRP6) co-receptors causes the formation of signalosomes at the plasma membrane and local inhibition of GSK3 (Bilić et al., 2007; Niehrs, 2012). The receptor complex is then endocytosed together with other cytoplasmic proteins such as Disheveled (Dvl), Axin1, and GSK3 (Taelman et al., 2010; Kim et al., 2015). The local decrease of GSK3 activity in signalosomes rapidly triggers macropinocytosis and internalization of the receptor complex, GSK3, and Axin1 (Tejeda-Muñoz et al., 2019). These are rapidly trafficked into late endosomes and, via the endosomal sorting complexes required for transport (ESCRT) machinery, inside the intraluminal vesicles of multivesicular bodies (MVBs) (Taelman et al., 2010; Dobrowolski et al., 2012; Albrecht et al., 2018). The sequestration of GSK3 and Axin is necessary for the stabilization of β-catenin (Taelman et al., 2010). The decrease of GSK3 in the cytosol results in the stabilization of many other GSK3 substrate proteins in a novel pathway known as Wnt stabilization of proteins (Wnt-STOP) (Kim et al., 2009; Taelman et al., 2010; Acebron et al., 2014).

Within a few minutes of adding Wnt3a protein, endocytic vesicles are formed (Tejeda-Muñoz et al., 2019; Albrecht et al., 2020). These vesicles correspond to MVBs and contain GSK3 that becomes protected from proteinase K digestion inside membrane-bounded organelles after permeabilizing the plasma membrane with digitonin (Albrecht et al., 2018). Wnt treatment triggers a large increase of non-receptor-mediated endocytosis of molecules such as BSA and high molecular weight Dextran (Albrecht et al., 2018; Tejeda-Muñoz et al., 2019), consistent with the view that Wnt signaling induces sustained macropinocytosis. Macropinocytosis is a non-receptor-mediated actin-driven process resulting from activation of p21-activated kinase-1 (Pak1) (Doherty and McMahon, 2009). This cell drinking mechanism leads to the formation of plasma membrane ruffles, actin tent poles, and macropinocytic cups that internalize extracellular fluid in vesicles of sizes 200 nm to 5 μm (Condon et al., 2018; Swanson and King, 2019). Macropinocytosis is driven by mechanisms very similar to those of phagocytosis, an ancient process that frequently involves integrins (Mylvaganam et al., 2021). On the other hand, receptor-mediated endocytosis leads to the formation of small vesicles of less than 100 nm visible only by electron microscopy mediated by the clathrin or caveolin machinery in a process-designated micropinocytosis (Nichols and Lippincott-Schwartz, 2001; Doherty and

[1]Department of Biological Chemistry, David Geffen School of Medicine, University of California, Los Angeles 90095-1662, USA

[2]Dipartimento di Scienze Chimiche, della Vita e della Sostenibilità Ambientale, University of Parma, Parm, Italy

[3]JT Biohistory Research Hall, Osaka, Japan and Chuo University, Faculty of Science and Engineering, Tokyo, Japan

[4]Department of Molecular, Cellular and Developmental Biology, University of California, Los Angeles, CA 90095-1662, USA

[5]Lead contact

*Correspondence: ntejedamunoz@mednet.ucla.edu (N.-M.), ederobertis@mednet.ucla.edu (E.M.D.R.)

https://doi.org/10.1016/j.isci.2022.104123

McMahon, 2009). In the case of Wnt-induced macropinocytosis, internalized macromolecules are rapidly trafficked into lysosomes where they are degraded, leading to changes in metabolism (Albrecht et al., 2020).

The starting point of the present investigation came when we noticed that the large cytoplasmic vesicles induced by Wnt3a were formed in the periphery of cultured cells, mainly at the leading edge. This is also the location of focal adhesion (FA) proteins which mediate the interaction between the cytoskeleton and the extracellular matrix (ECM) via integrins (Abercrombie et al., 1971; Bachir et al., 2017). This localization reminded us of intriguing results presented by Capelluto et al. (2002) in which they described that overexpressed Dvl protein, which is also a component of Wnt MVBs, was found in actin cables and cytoplasmic puncta. Although not specified at the time, in their images the puncta were frequently located at the tip of actin cables which is also the location of FAs (Capelluto et al., 2002). This led us to hypothesize that FAs and integrins might crosstalk with Wnt signaling.

In the present paper, we show that within 20 min of Wnt3a addition, human fibroblasts and cultured cell lines underwent major rearrangements of the actin cytoskeleton and focal adhesions. Using cell surface biotinylation, we showed that Wnt3a treatment leads to the internalization of Integrin β1 (ITGβ1). Proteinase K protection studies *in situ* revealed that ITGβ1 and other FA proteins, such as zyxin and Src, were sequestered in MVBs after Wnt3a treatment. Finally, a sensitized *Xenopus* embryo assay showed that ITGβ1 depletion decreased phenotypes caused by overexpressed *Wnt8* mRNA, and that this effect was rescued by human *ITGβ1* mRNA. Taken together, the results suggest an unexpected connection between focal adhesions, integrins, and canonical Wnt signaling.

RESULTS

Wnt3a causes a major rearrangement of the actin cytoskeleton and focal adhesions in human corneal stromal (HCSF) fibroblasts

Wnt signaling causes the uptake of large amounts of extracellular fluid by macropinosomes (Redelman-Sidi et al., 2018; Tejeda-Muñoz et al., 2019). In addition, a gene ontology analysis of biotinylated Wnt-induced Lrp6-APEX2 target proteins indicated that LRP6-interacting proteins were involved in actin cytoskeleton remodeling (Colozza et al., 2020). To examine whether Wnt induced changes in the cytoskeleton, primary human corneal stromal (HCSF) fibroblasts (Gallego-Muñoz et al., 2018) were treated with Wnt3a. Fibroblasts showed abundant vinculin FA sites at the tip of F-actin cables, particularly in the leading edge of the cell (Figures 1A–1A″). Wnt treatment caused the loss of focal adhesion sites within 20 min (Figures 1B–1B″). This indicated that the cytoskeleton responds to Wnt stimulation through a loss of FAs.

Cancer cells undergo certain fundamental changes in terms of cell physiology to attain a malignant phenotype. Loss of cell-cell adhesion is caused by changes in the expression of adhesion proteins, which plays an important role in infiltration and metastasis (Bachir et al., 2017). To investigate how the Wnt pathway affects cell adhesion and motility, we used hepatocellular carcinoma (HCC) Alexander1 ± Axin1 cells (Albrecht et al., 2020). This HCC cell line has a deletion in the GSK3 binding region of the tumor suppressor Axin1, resulting in the constitutive activation of the Wnt pathway. A stable permanent cell line derivative that restores full-length Axin1 at physiological levels (Albrecht et al., 2020) serves as a control for the effect of Axin1 mutation. We filmed cells by differential interference contrast (DIC) light microscopy and found that mutation of Axin1 dramatically affected membrane motility, consistent with an increase in macropinocytosis (Figure S1A). Video S1 shows that mutation in Axin1 causes extensive membrane ruffling and macropinocytosis in HCC cells (related to Figures 1 and S1). This was manifested as wave-like extensions of the lamellipodium and extensive ruffling of the plasma membrane; when Axin1 was restored, membrane ruffling was lost (Video S1). In a similar way, dissociated *Xenopus* animal cap cells injected with membrane GFP and Lifeact mRNA (marking F-actin) and cultured on fibronectin showed macropinocytic membrane ruffles within 20 min of addition of LiCl, a treatment that mimics Wnt signaling by inhibiting GSK3 (Figures S1B–S1B′). Video S2 shows that mimicking Wnt with the GSK3 inhibitor LiCl triggers macropinocytic cup formation in cultured *Xenopus* animal cap cells (related to Figures 1 and S1). The circular membrane ruffling movements seen in animal cap cells were very similar to those caused by transfection of oncogenic HRas (G12V mutation), a classical inducer of macropinocytosis (Ramirez et al., 2019) in transfected 3T3 fibroblasts (Figures S1C–S1C′). Video S3 shows that activated Ras-GFP triggers macropinocytosis (related to Figures 1 and S1). The results indicate that Wnt signaling has major effects on the actin cytoskeleton, leading to loss of focal adhesions. This is accompanied by extensive membrane ruffling activity characteristic of macropinocytosis.

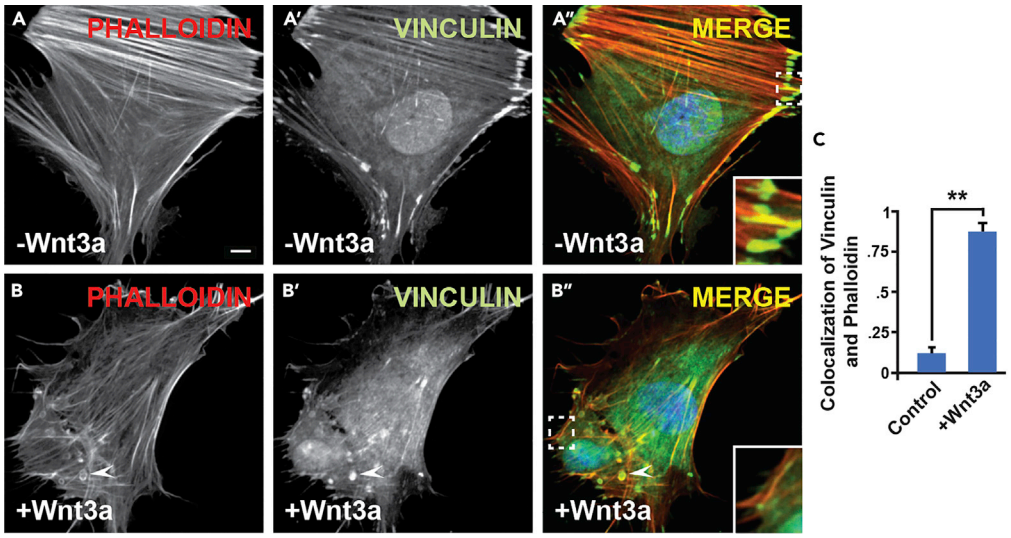

Figure 1. Wnt3a treatment for 20 min causes a major rearrangement of the actin cytoskeleton and focal adhesions in human corneal stromal (HCSF) fibroblasts

(A-A″) Image of HCSF fibroblast showing that the cells attach well to fibronectin-coated plastic, have prominent F-actin cables stained by Phalloidin (in red), and abundant focal adhesion sites immunostained with vinculin (in green).

(B-B″) Wnt3a treatment causes disorganization of the actin cytoskeleton, vinculin becomes associated with intracellular vesicles sometimes surrounded by F-actin (indicated by arrowheads), and few focal adhesions are visible. Similar results were obtained in three independent experiments. Insets show higher magnifications of actin and vinculin colocalization. Nuclei were stained with DAPI. Scale bars, 10 μm.

(C) Quantification of the colocalization of vinculin and the F-actin marker phalloidin by Pearson's correlation coefficient using ImageJ. Error bars denote SEM ($n \geq 3$) (**$p < 0.01$). See also Figure S1 and Videos S1–S4.

Canonical Wnt signaling induces membrane vesicles at focal adhesions

Capelluto et al. reported that the DIX domain of Disheveled is associated with actin cables and vesicular structures (Capelluto et al., 2002). We found it interesting that the membrane vesicles formed preferentially at the ends of actin cables, and hypothesized these might correspond to FAs. When HeLa cells were treated with Wnt3a for 20 min, puncta visible by DIC were formed at the leading edge of the cell (Figures 2A–2D′, indicated with arrowheads). These vesicles had concentrated endogenous GSK3, a protein normally uniformly distributed in the cytosol (Figures 2A′ and 2B′). Importantly, the Wnt-induced vesicles contained the FA protein zyxin (Beckerle, 1986). Wnt-induced GSK3 and zyxin-containing vesicles were quantified in Figures 2E and 2F. Overexpression of transfected CA-LRP6-GFP lacking the extracellular domain, elicits a potent Wnt signal mediated by the formation of MVBs (Taelman et al., 2010), and also caused colocalization with endogenous zyxin (Figure S2). The results indicate that Wnt signaling causes the endocytosis of focal adhesion proteins into the same vesicles that sequester GSK3, suggesting a connection between the Wnt pathway and the focal adhesion signaling pathway.

Plasma membrane Integrin β-1 is rapidly endocytosed after Wnt treatment

Integrins are constantly endocytosed and recycled back to the plasma membrane through multiple pathways (Moreno-Layseca et al., 2019; Li et al., 2020). Tight regulation of integrin turnover from the cell surface is pivotal to a number of biological processes. This includes cell migration, cytokinesis, and cancer cell invasion and metastasis. Integrins are predominantly endocytosed via clathrin-mediated endocytosis (CME), but other mechanisms such as caveolin and macropinocytosis have also been implicated (Gu et al., 2011; Moreno-Layseca et al., 2019).

To examine whether Wnt3a affected the endocytosis of ITGβ1, a surface biotinylation assay was performed (Figure 3). HeLa cells were treated with Wnt3a protein on ice or incubated at 37°C for 15 or 30 min before placing on ice (low temperature prevents endocytosis), and the plasma membrane was labeled with non-cell permeable sulfo-NHS-SS-Biotin for 30 min. Biotinylated proteins were pulled down with streptavidin-agarose beads followed by a western blot with ITGβ1 antibody. Wnt3a treatment resulted in a rapid depletion of ITGβ1 from the cell surface (Figure 3, compare lane 6 to lanes 7 and 8). Transferrin receptor (TfR),

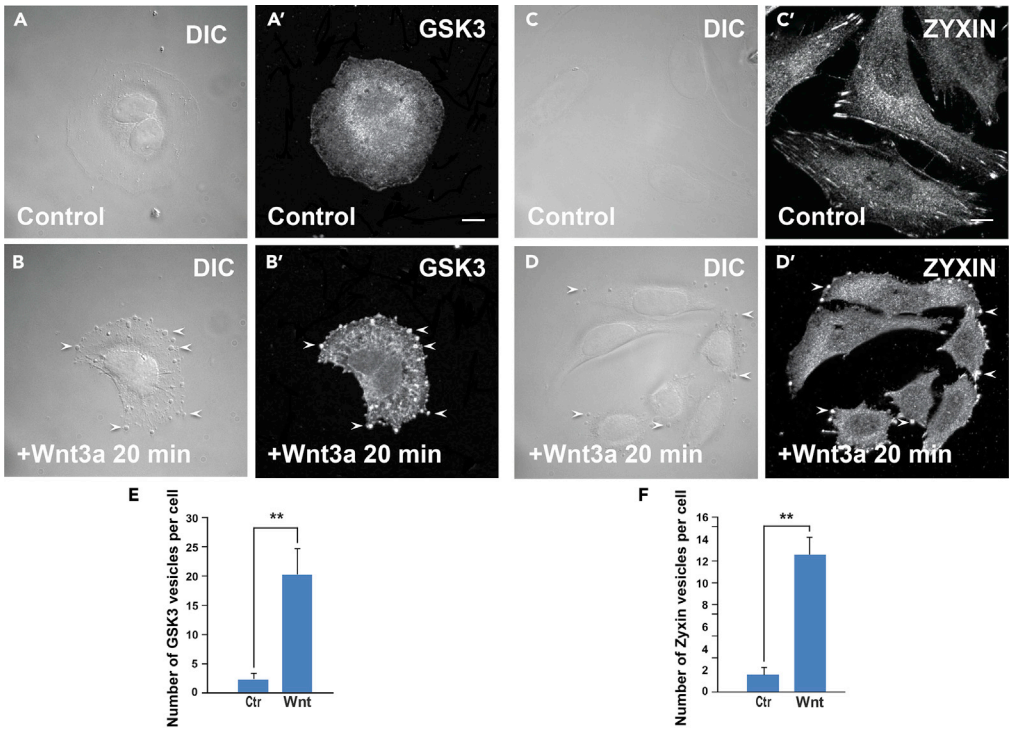

Figure 2. Wnt3a treatment caused the formation of vesicles that sequestered GSK3 and the focal adhesion protein zyxin; Immunostainings of endogenous GSK3 and zyxin

(A–B′) Fluorescence microscopy images in HeLa cells showing that Wnt treatment (100 ng/mL, 20 min) caused the translocation of GSK3 from the cytosol into vesicles. Note that Wnt3a protein caused the formation of prominent vesicles visible by light microscopy (arrowheads).

(C–D′) The focal adhesion protein zyxin is sequestered in vesicles, as GSK3 is, by 20 min Wnt stimulation. Images were generated using a Zeiss Imager Z.1 microscope with Apotome using high magnification.

(E–F) Quantification of the immunofluorescence found in vesicles (see STAR Methods). Scale bars, 10 μm. Error bars denote SEM ($n \geq 3$) (**$p < 0.01$). See also Figure S2.

which is recycled independently of the Wnt pathway, was used as a plasma membrane control, and remained unchanged. We conclude that Wnt3a treatment induces acute endocytosis of ITGβ1 from the cell surface; given the rapid time course, this is unlikely to be through transcriptional mechanisms.

To investigate whether the sustained activation of the Wnt pathway that occurs in cancer cells also alters focal adhesions, we used the Alexander1 HCC ± Axin1 system, which carries a mutation in the GSK3 binding site of Axin1 (Albrecht et al., 2020). RNAseq genome set enrichment analyses (GSEA) showed that mutation of Axin1 strongly affected the BioCarta Integrin pathway set of 34 genes, leading to a reduction in the transcript levels of Talin 1 (TLN1) and Integrin-β1 when compared to cells in which Axin1 had been reconstituted (Figure S3A, arrowhead). This result was confirmed by immunostaining of HCC ± Axin1 cells on fibronectin-coated slides, which showed that while abundant ITGβ1 focal adhesions were present in cells reconstituted with wild-type Axin1, they were greatly reduced in Axin1 mutant cells (Figures S4B and S4C). We conclude that in a cancer cell model, sustained activation of the Wnt pathway by mutation of a tumor suppressor strongly reduces ITGβ1 and focal adhesions at a transcriptional level, in addition to the rapid Wnt-induced clearing of Integrin β-1 by endocytosis.

GSK3 and ITGβ1 are protected from protease digestion inside MVBs after Wnt3a treatment

The gold standard for determining the localization of a protein inside a membrane-bounded compartment is the protease protection assay (Vanlandingham and Ceresa, 2009). To test whether focal adhesion proteins were translocated inside membrane vesicles after Wnt3a treatment, we used HeLa cells permeabilized with digitonin. Digitonin solubilizes patches of the cholesterol-rich plasma membrane but leaves intracellular membranes unaffected (see diagram in Figure 4A). Cells were treated ± Wnt3a, placed on

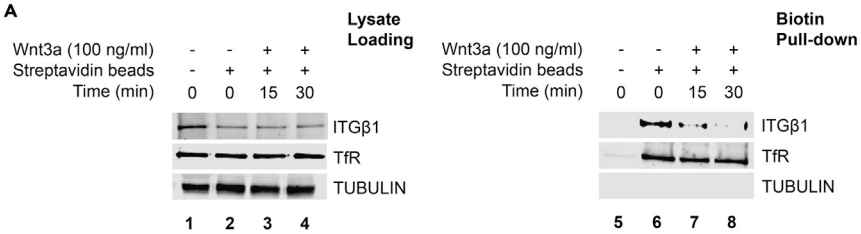

Figure 3. Integrin beta-1 is rapidly endocytosed by Wnt

Time course (0–30 min) of Wnt3a treatment was performed in HeLa cells at a permissive temperature for endocytosis. After that, the plasma membrane was labeled with Sulfo-NHS-SS-Biotin on ice for 30 min. Pull-down assay with streptavidin-agarose beads showed that Wnt treatment induced the endocytosis of ITGβ1 after 15 min. Lanes 1–4 are HeLa Cell lysate loading controls. Lanes 5–8 show samples after pull-down with biotin agarose beads. Cell extracts were analyzed by western blot with ITGβ1 antibody. Note that cell surface ITGβ1 is endocytosed after 15 or 30 min of Wnt3a treatment. Transferrin Receptor (TfR) was used as a specificity control that is recycled independently of the Wnt pathway. Tubulin antibodies served as a control for cytoplasmic contamination. Similar results were obtained in three independent experiments. See also Figure S3.

ice, and permeabilized *in situ* with digitonin (Albrecht et al., 2018). The addition of Proteinase K degraded cytosolic proteins (Figure 4B), but in Wnt-treated cells, ITGβ1 and GSK3 were protected from protease digestion inside common vesicles (compare Figure 4C, arrowheads). These puncta corresponded to membrane-bounded organelles, since treatment with 0.01% Triton X-100, which dissolves all intracellular membranes, eliminated the protease protection of ITGβ1 and GSK3 (Figures 4D and 4E).

We next tested whether another component of the focal adhesion pathway, c-Src, was also endocytosed in ITGβ1-containing vesicles. We chose c-Src because it is an important proto-oncogene tyrosine kinase, known to regulate the cytoskeleton and the disassembly of focal adhesions in its activated form (Kaplan et al., 1994; Frame et al., 2002). When the proteinase K protection assay was performed using an anti-phospho-c-Src antibody that marks phosphorylated Tyr416 in the activation loop, it was found that Wnt3a treatment also relocalized c-Src into Wnt-induced membrane vesicles that contained GSK3 (Figure S4).

To determine whether the protease-protected organelles corresponded to MVBs, we used vacuolar protein sorting 4 (Vps4) labeled with GFP. Vps4 is an ATPase component of the ESCRT machinery required in the final stages of pinching off intraluminal vesicles (Gruenberg and Stenmark, 2004). A very useful reagent is provided by a point mutation in the ATP binding site, called VPS4-EQ, which generates a potent dominant-negative protein that prevents MVB formation and Vps4 localization to MVBs (Tejeda-Muñoz et al., 2019). Untreated HeLa cells transiently transfected with wild-type Vps4-GFP showed MVBs that did not colocalize strongly with ITGβ1 focal adhesions (Figure 5A). However, in cells treated with Wnt3a for 20 min, Vps4-GFP relocated to ITGβ1-containing puncta (Figure 5B, arrowheads). Transfected dominant-negative Vps4-EQ showed that ITGβ1 did not overlap with Vps4-EQ-GFP, both in the absence or presence of Wnt3a, providing a specificity control for MVB localization (Figures 5C and 5D).

We conclude that after short Wnt treatments, Integrin β-1 is relocalized from focal adhesions to membrane-bounded organelles that contain GSK3. In addition, the proto-oncogene c-Src, which promotes focal adhesion disassembly, was also translocated into these vesicles. The Wnt-induced puncta corresponded to multivesicular bodies containing the wild-type form of the ESCRT marker Vps4.

ITGβ1 MO reduces Wnt signaling

To investigate whether ITGβ1 has a crosstalk with Wnt signaling, we used *Xenopus* embryos, which are widely used as a Wnt assay system (Niehrs, 2022). We developed a sensitized system in which microinjection of 0.5 pg of *xWnt8* mRNA into the animal pole of each 4-cell stage blastomere consistently resulted in the complete dorsalization of the embryo, leading to development into radial head structures (Figures 6A and 6B). We designed an ITGβ1 antisense morpholino (MO) oligonucleotide. When injected on its own, ITGβ1 MO was without phenotypic effect (Figure 6C), but when co-injected together with xWnt8 it reduced dorsalization and allowed for the formation of partial axial structures (Figure 6D). This decrease in Wnt-induced signaling was specific for ITGβ1 depletion, as it was restored by microinjection of human ITGβ1

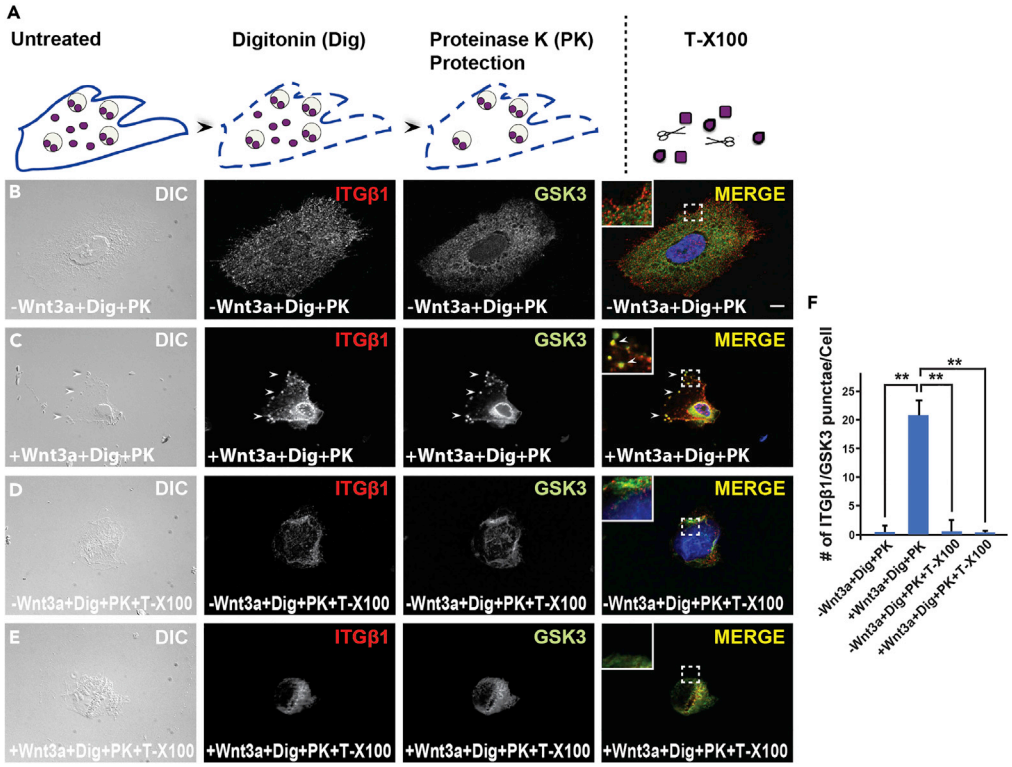

Figure 4. GSK3 and Integrin β-1 are protected from proteinase K digestion inside membrane-bounded organelles in digitonin-permeabilized cells, but not in the presence of Triton X-100 which solubilizes intracellular membranes

(A) Diagram of steps involved in the *in situ* protease protection assay.

(B and C) HeLa cells plated on glass coverslips were permeabilized with digitonin, treated with proteinase K to digest cytosolic proteins, stained with ITGβ1 and GSK3 antibodies, and analyzed by fluorescence microscopy. ITGβ1 and GSK3 were protease-protected within the same vesicles after treatment with Wnt3a protein for 20 min.

(D and E) HeLa cells treated as described above, except for the addition of Triton X-100, used as control, which dissolves inner membranes and leads to the digestion by exogenous protease of ITGβ1 and GSK3; DAPI labels nuclei. All of the assays were performed in triplicate. Insets show higher magnification views. Scale bars, 10 μm.

(F) Quantification of the number of puncta double-stained with ITGβ1 and GSK3 antibodies in protease protection assay using ImageJ. Error bars denote SEM ($n \geq 3$) (**$p < 0.01$). See also Figure S4.

mRNA that differs in the MO-targeted region (Figures 6E and 6F). The Wnt signaling embryo assay differs from the more familiar secondary axis induction assay in which radial head structures lacking trunk are induced (compare Figures 6B–6H). In *Xenopus* animal cap reporter gene assays, overexpression of a human dominant-negative ITGβ1 construct (Retta et al., 1998) inhibited β-catenin signaling when compared to wild-type hITGβ mRNA (Figure S5). The results indicate that cell adhesions to the cell matrix via ITGβ1 facilitate Wnt signaling in the context of the *Xenopus* embryo.

DISCUSSION

The main finding in this study was that a crosstalk exists between canonical Wnt signaling and focal adhesions. As shown in Figure 7, binding of Wnt to its receptors Lrp6 and Frizzled causes a local inhibition of GSK3 activity, an enzyme that normally inhibits macropinocytosis mediated by the cellular actin machinery in the leading edge lamellipodium (Tejeda-Muñoz et al., 2019; Albrecht et al., 2020). The receptor complex is rapidly endocytosed into late endosomes/MVBs that fuse with lysosomes which become more acidic, degrading macropinocytosed macromolecules (Albrecht et al., 2021). The sequestration of GSK3 inside the endosomal compartment via the ESCRT machinery is required for sustained canonical Wnt signaling (Taelman et al., 2010; Vinyoles et al., 2014; Tejeda-Muñoz et al., 2019). Our attention was drawn to focal adhesions by a study showing that a Wnt pathway component, Disheveled, associated with membrane vesicles that localized to the end of actin cytoskeletal cables (Capelluto et al., 2002), which is also the location of

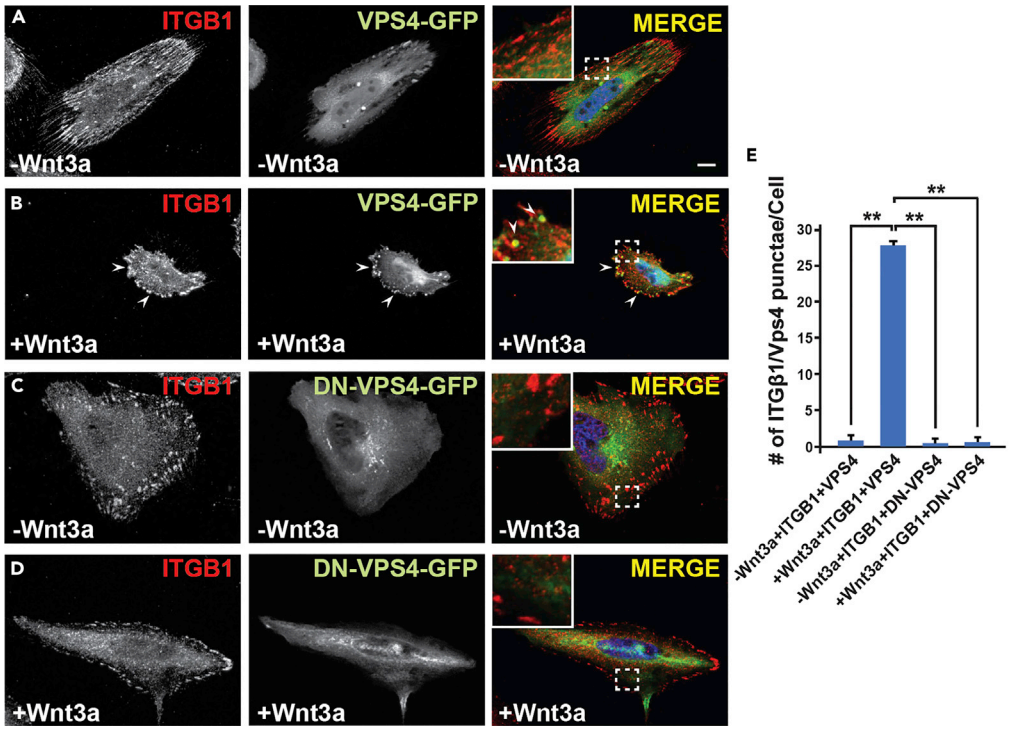

Figure 5. Integrin β-1 colocalizes together with the multivesicular endosome marker Vps4, but not with its dominant-negative point mutant Vps4-EQ

(A and B) HeLa cells transiently transfected with Vps4-GFP were analyzed using fluorescence microscopy with anti- ITGβ1 antibody. Wnt3a treatment of 20 min caused the re-distribution of ITGβ1 into puncta, known to correspond to MVBs (-Taelman et al., 2010), indicated by arrowheads.

(C and D) Overexpression of the dominant-negative-Vps4-GFP construct containing a single mutation (EQ) in the ATP binding site blocked the induction of ITGβ1 vesicles by Wnt protein. All assays were performed in triplicate. Scale bars, 10 μm.

(E) Quantification of ITGβ1 and Vps4 double-positive puncta in transfected HeLa cells. Error bars denote SEM ($n \geq 3$) (**$p < 0.01$).

focal adhesions. Primary fibroblasts rearrange the cytoskeleton within 20 min of Wnt3a addition, and the focal adhesion marker vinculin became internalized (Figure 1). In HeLa cells, Wnt addition caused the formation of prominent vesicles visible by DIC brightfield; these vesicles colocalized with GSK3 and the focal adhesion marker zyxin (Figure 2). Integrins are transmembrane proteins that anchor the actin cytoskeleton to the extracellular matrix. Consisting of α and β subunits, there are 24 possible heterodimers, yet the majority share a common β-1 subunit, leading us to focus on ITGβ1 (Moreno-Layseca et al., 2019). Cell surface biotinylation studies showed that ITGβ1 protein was endocytosed within 15–30 min of Wnt3a treatment (Figure 3, lanes 6–8). *In situ* protease protection studies showed that after Wnt signaling ITGβ1 became relocalized to membrane-bounded organelles that were the same ones that sequestered GSK3 (Figure 7). These vesicles were specifically labeled by the MVB marker Vps4 and therefore corresponded to MVBs. An important regulator of focal adhesion disassembly, the proto-oncogene c-Src (Moreno-Layseca et al., 2019), was also relocalized inside Wnt-induced membrane-bounded organelles (Figure S4). These experiments suggest that, unexpectedly, Wnt-induced endocytosis resulted in the translocation of multiple focal adhesion components into late endosomes.

The downregulation of FAs and ITGβ1 by both transcriptional and non-transcriptional mechanisms raises the possibility that Wnt signaling might induce an epithelial-mesenchymal transition (EMT) program. Consistent with this view, in animal cap cells, GSK3 inhibition with LiCl rapidly induced not only macropinocytosis but also directional cell migration. Video S4 shows increased cell motility triggered in *Xenopus* animal cap cells by the GSK3 inhibitor LiCl, which mimics Wnt signaling (related to Figures 1 and S1). The repression of Cadherin transcription is a hallmark of EMT (Nieto et al., 2016). In a sustained activation

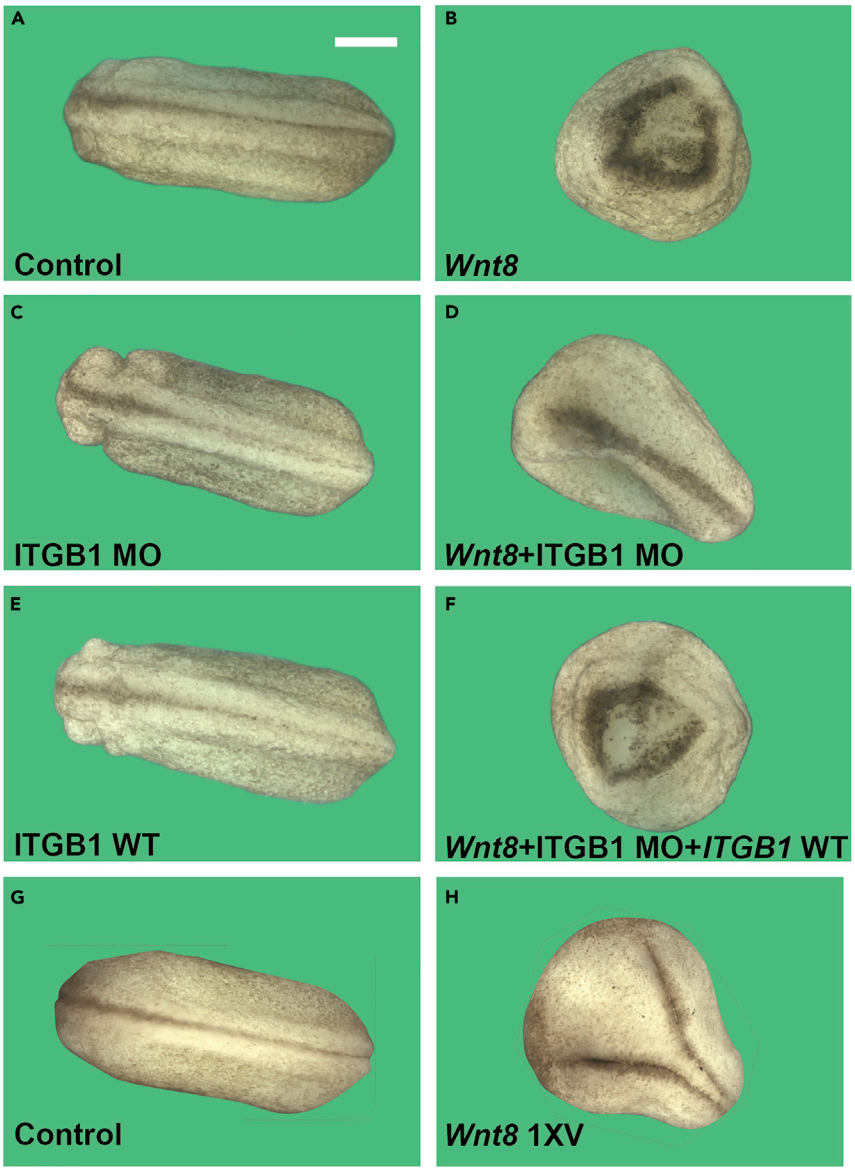

Figure 6. ITGβ1 MO inhibits Wnt signaling in a sensitized *Xenopus* embryo assay in which injection of *xWnt8* four times into the animal pole induces a radial dorsalized phenotype

(A) Control *Xenopus* embryos at early tail bud.

(B) Embryos injected four times in the animal region at the 4-cell stage with 0.5 pg *Wnt8myc* mRNA consistently induced a radial head phenotype lacking any trunk development.

(C) No phenotype was observed with ITGβ1 MO alone.

(D) Co-injection of xITGβ1 antisense MO consistently inhibited the dorsalizing effects of xWnt8, allowing the formation of partial axial structures.

(E) Microinjection of human *ITGβ1* mRNA was without phenotypic effect.

(F) The effect of ITGβ1 MO was specific because it was rescued by human *ITGβ1* mRNA which is not targeted by the MO sequence.

(G and H) Injecting the same dose (0.5 pg) of *xWnt8myc* mRNA into a single ventral marginal location in 4-cell embryos induces the familiar axis duplication phenotype; it is shown here to contrast with the radial dorsalized phenotype caused by four injections into the animal pole used in this sensitized assay system. Images were taken with an Axio Zoom V.16 Stereo Zoom Zeiss at low magnification. Similar results were obtained in five independent experiments. Numbers of embryos analyzed were as follows A = 140, 100%; B = 128, 97%; C = 132, 98%; D = 125, 92%; E = 129, 100%; F = 124, 85% (5 independent experiments); G = 48, 100%; H = 92, 91% complete axes (2 independent experiments). Scale bar, 500 μm. For β-catenin reporter assay in animal caps, see Figure S5.

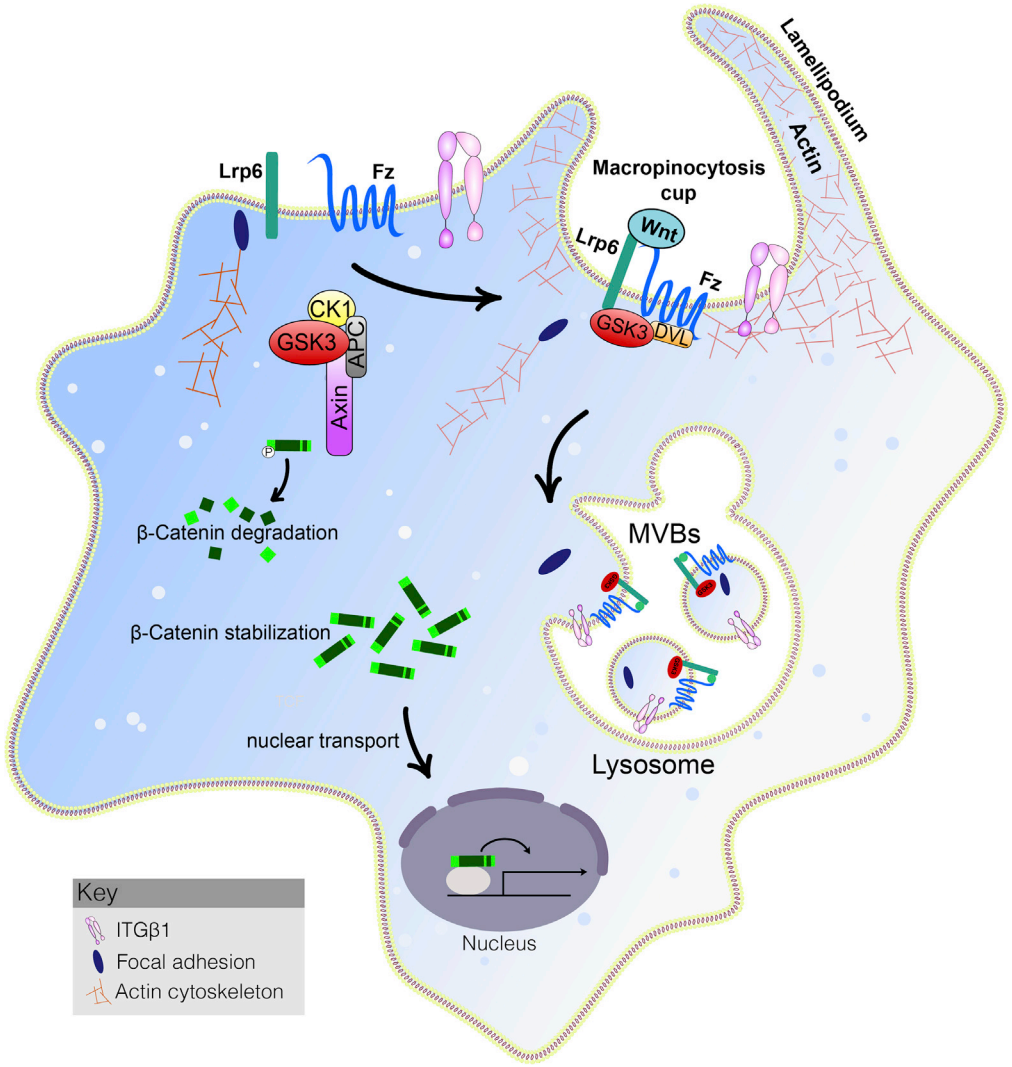

Figure 7. Model of the endocytosis of the focal adhesion and ITGβ1 by Wnt

After Wnt treatment, Lrp6/Fz/Wnt/GSK3 signalosomes, the master regulator of cell adhesion ITGβ1, and other focal adhesion components are endocytosed by macropinocytic cups in an actin-driven process. Macropinocytosis is required for canonical Wnt signaling. Sequestration of GSK3 in MVBs is necessary for the stabilization of β-catenin that mediates the transcriptional activity of canonical Wnt.

situation, HCC Alexander cells that are mutated in the GSK3 binding site of Axin1 (Albrecht et al., 2020), reconstitution with wild-type Axin1 resulted in an increase of cadherin 1 (CDH1, also known as E-cadherin) transcripts (GEO Accession Number GSE193381). CDH1 is the main cadherin expressed in these cells. This CDH1 transcript upregulation by wild-type Axin1 mirrored the increase in Integrin-β1 focal adhesions observed by immunostaining (Figures S3B and S3C). The increase in cadherin 1 transcripts was 41% and, given that the RNAseq was carried out in quadruplicate, was highly significant (adjusted p-value 0.003). The EMT-promoting transcription factor Twist2 (Nieto et al., 2016) was also significantly affected (adjusted P-value 00,005), showing a decrease of 62% in HCC cells reconstituted with Axin1. The relationship between plasma membrane macropinocytosis, directional cell movement, integrins, cadherins, and the EMT program merits further investigation.

Previous indications existed in the literature suggesting interactions between FAs and Wnt signaling, which are two major pathways of cellular transduction. For example, it has been reported that extracellular matrix stiffness causes increased transcription of Wnt1 through the activation of the integrin-focal adhesion kinase

(FAK) pathway (Du et al., 2016). The focal adhesion protein Kindlin-2, was found to directly bind to β-catenin and TCF4 forming a transcriptional complex that enhances Wnt signaling in tumors (Yu et al., 2012). Recent studies on cell polarization and migration have shown that key elements in the Wnt pathways such as GSK3 are essential to cell polarity. GSK3 influences cell migration as one of the regulators of the spatiotemporally controlled dynamics of the actin cytoskeleton, microtubules, and cell-to-matrix adhesions (Sun et al., 2009). In this regard, it has been reported that GSK3 phosphorylates FAK, reducing its activity and consequently impeding cell spreading and migration (Bianchi et al., 2005). In contrast, other experiments indicate that GSK3 promotes cell spreading by phosphorylating paxillin, a focal adhesion constituent (Cai et al., 2006). It is known that the tyrosine kinase c-Src, which participates in focal adhesion disassembly, also binds to and phosphorylates Disheveled 2, dampening Wnt transcriptional signals (Yokoyama and Malbon, 2009).

The ESCRT machinery has been shown to regulate the transit of c-Src from endosomes to the plasma membrane, promoting the turnover of cell-ECM adhesions during cell migration (Tu et al., 2010). In our experiments, the ESCRT machinery was shown to be involved in the endocytosis of ITGβ1 as well as that of c-Src. In an interesting recent study, it was found that macropinocytosis serves as a novel mechanism that shuttles actin to the leading edge for lamellipodium expansion during neural crest migration (Li et al., 2020).

Although there are multiple examples of interactions between Wnt and focal adhesions in the literature, the results presented here differ in that we discovered that focal adhesions are rapidly translocated into MVB vesicles after Wnt signaling. Furthermore, using a sensitized *Xenopus* embryo assay in which microinjection of *xWnt8* mRNA caused completely radial embryos consisting of heads and no tails, we found that depletion of ITGβ1 attenuated the effects of Wnt overexpression (Figure 6). This suggests that in the context of the cellular architecture of the embryo, focal adhesions to the cell matrix facilitate cell-cell Wnt signaling. Because Wnt downregulates focal adhesions and integrin depletion dampens Wnt signaling, the two pathways might establish a negative feedback loop that limits the duration of Wnt signals.

The transition from single-celled to multicellular organisms marked the emergence of complex life forms. Understanding molecular and cellular mechanisms of key cell signaling pathways in both development and disease has been a major focus of research. The Wnt and integrin signaling pathways are very ancient and were already present in sponges (Brower et al., 1997; Loh et al., 2016). Wnt signaling drives a cell growth program that can become inappropriately activated in cancer. Wnt and cell adhesion are often active in the same developmental processes and crosstalk between them should result in reciprocal regulation. Knowing how Wnt signaling and focal adhesions cooperate will improve our understanding of embryonic development and tumorigenesis. Cancer therapies in the past have focused on blocking the uncontrolled cell division of primary tumors. However, almost all cancer deaths are due to metastatic cancer, not primary tumors. We uncovered here a new regulation model by which Wnt signaling changes cell adhesion through endocytosis of focal adhesion components. It has been proposed that focal adhesion restoration strategies could be useful in the treatment of metastatic cancer (Griffith et al., 2005; Li et al., 2016; Chaturvedi et al., 2014; Ramirez et al., 2011). Understanding how macropinocytosis, Wnt, and focal adhesions intersect could lead to new targets in cancer treatment.

Limitations of the study

A limitation of this work is that the effect of the role of focal adhesions in Wnt signaling was not investigated in mammalian cells. The effect of integrin in promoting Wnt signaling was only tested in the context of the frog embryo. In the future, it will be important to analyze the effect of integrin depletion on Wnt signaling in culture cells on hard and soft integrin-interacting substrates.

STAR★METHODS

Detailed methods are provided in the online version of this paper and include the following:

- KEY RESOURCES TABLE
- RESOURCE AVAILABILITY
  - Lead contact
  - Materials availability
  - Data and code availability

SUPPLEMENTAL INFORMATION

Supplemental information can be found online at https://doi.org/10.1016/j.isci.2022.104123.

ACKNOWLEDGMENTS

We are grateful to D. Geissert for technical assistance, H. Coller for human corneal fibroblasts, R. Moon for BAR reporters, J. Monka and Y. Ding for comments on the manuscript, and M. F. Domowicz for help with the illustrations. Funding bodies were UC Cancer Research Coordinating Committee (grant C21CR2039); National Institutes of Health grant P20CA016042 to the University of California, Los Angeles Jonsson Comprehensive Cancer Center; and the Norman Sprague Endowment for Molecular Oncology.

AUTHOR CONTRIBUTIONS

N.T.M. designed research; N.T.M., Y.M., P.S., M.M., M.P., and E.M.D.R. performed research and analyzed data; N.T.M. and E.M.D.R. wrote the paper.

DECLARATION OF INTERESTS

The authors declare no competing interests.

Received: January 25, 2022
Revised: February 14, 2022
Accepted: March 16, 2022
Published: April 15, 2022

REFERENCES

Abercrombie, M., Heaysman, J.E., and Pegrum, S.M. (1971). The locomotion of fibroblasts in culture. IV. Electron microscopy of the leading lamella. Exp. Cell Res. *67*, 359–367. PMID: 5097522. https://doi.org/10.1016/0014-4827(71)90420-4.

Acebron, S.P., Karaulanov, E., Berger, B.S., Huang, Y.L., and Niehrs, C. (2014). Mitotic Wnt signaling promotes protein stabilization and regulates cell size. Mol. Cell *54*, 663–674. PMID: 24837680. https://doi.org/10.1016/j.molcel.2014.04.014.

Albrecht, L.V., Ploper, D., Tejeda-Muñoz, N., and De Robertis, E.M. (2018). Arginine methylation is required for canonical Wnt signaling and endolysosomal trafficking. Proc. Natl. Acad. Sci. U S A. *115*, E5317–E5325. PMID: 29773710. https://doi.org/10.1073/pnas.1804091115.

Albrecht, L.V., Tejeda-Muñoz, N., Bui, M.H., Cicchetto, A.C., Di Biagio, D., Colozza, G., Schmid, E., Piccolo, S., Christofk, H.R., and De Robertis, E.M. (2020). GSK3 inhibits macropinocytosis and lysosomal activity through the Wnt destruction complex machinery. Cell Rep. *32*, 107973. PMID: 32726636. https://doi.org/10.1016/j.celrep.2020.107973.

Albrecht, L.V., Tejeda-Muñoz, N., and De Robertis, E.M. (2021). Cell biology of canonical Wnt signaling. Ann. Rev. Cell Dev. Biol. *37*, 369–389. PMID: 34196570. https://doi.org/10.1146/annurev-cellbio-120319-023657.

Bachir, A.I., Horwitz, A.R., Nelson, W.J., and Bianchini, J.M. (2017). Actin-based adhesion modules mediate cell interactions with the extracellular matrix and neighboring cells. Cold Spring Harb. Perspect. Biol. *9*. PMID: 28679638. https://doi.org/10.1101/cshperspect.a023234.

Beckerle, M.C. (1986). Identification of a new protein localized at sites of cell-substrate adhesion. J. Cell Biol. *103*, 1679–1687. PMID: 3536951. https://doi.org/10.1083/jcb.103.5.1679.

Bianchi, M., De Lucchini, S., Marin, O., Turner, D.L., Hanks, S.K., and Villa-Moruzzi, E. (2005). Regulation of FAK Ser-722 phosphorylation and kinase activity by GSK3 and PP1 during cell spreading and migration. Bioch. J. *391*, 359–370. PMID: 15975092. https://doi.org/10.1042/BJ20050282.

Bilić, J., Huang, Y.L., Davidson, G., Zimmermann, T., Cruciat, C.M., Bienz, M., and Niehrs, C. (2007). Wnt induces LRP6 signalosomes and promotes Dishevelled-dependent LRP6 phosphorylation. Science *316*, 1619–1622. PMID: 17569865. https://doi.org/10.1126/science.1137065.

Brower, D.L., Brower, S.M., Hayward, D.C., and Ball, E.E. (1997). Molecular evolution of integrins: genes encoding integrin β subunits from a coral and a sponge. Proc. Natl. Acad. Sci. U S A. *94*, 9182–9187. PMID: 9256456. https://doi.org/10.1073/pnas.94.17.9182.

Cai, X., Li, M., Vrana, J., and Schaller, M.D. (2006). Glycogen Synthase Kinase 3- and extracellular signal-regulated kinase-dependent phosphorylation of Paxillin regulates cytoskeletal rearrangement. Mol. Cell. Biol. *26*, 2857–2868. PMID: 16537926. https://doi.org/10.1128/MCB.26.7.2857-2868.2006.

Capelluto, D.G.S., Kutateladze, T.G., Habas, R., Finkielstein, C.V., He, X., and Overduin, M. (2002). The DIX domain targets Dishevelled to actin stress fibres and vesicular membranes. Nature *419*, 726–729. PMID: 12384700. https://doi.org/10.1038/nature01056.

Chaturvedi, A., Hoffman, L.M., Jensen, C.C., Lin, Y.C., Grossmann, A.H., Randall, R.L., Lessnick, S.L., Welm, A.L., and Beckerle, M.C. (2014). Molecular dissection of the mechanism by which EWS/FLI expression compromises actin cytoskeletal integrity and cell adhesion in Ewing sarcoma. Mol. Biol. Cell. *25*, 2695–2709. PMID: 25057021. https://doi.org/10.1091/mbc.E14-01-0007.

Chen, S., Zhou, Y., Chen, Y., and Gu, J. (2018). Fastp: an ultra-fast all-in-one FASTQ preprocessor. Bioinformatics *34*, i884–i890. PMID: 30423086. https://doi.org/10.1093/bioinformatics/bty560.

Colozza, G., Jami-Alahmadi, Y., Dsouza, A., Tejeda-Muñoz, N., Albrecht, L.V., Sosa, E., Wohlschlegel, J.A., and De Robertis, E.M. (2020). Wnt-inducible Lrp6-APEX2 interacting proteins identify ESCRT machinery and Trk-fused gene as components of the Wnt signaling pathway. Sci. Rep. *10*, 21555. PMID: 33299006. https://doi.org/10.1038/s41598-020-78019-5.

Condon, N.D., Heddleston, J.M., Chew, T.L., Luo, L., McPherson, P.S., Ioannou, M.S., Hodgson, L., Stow, J.L., and Wall, A.A. (2018). Macropinosome formation by tent pole ruffling in macrophages. J. Cell Biol. *217*, 3873–3885. PMID 30150290. https://doi.org/10.1083/Jcb.201804137.

Ding, Y., Colozza, G., Sosa, E.A., Moriyama, Y., Rundle, S., Salwinski, L., and De Robertis, E.M. (2018). Bighead is a Wnt antagonist secreted by the Xenopus Spemann organizer that promotes Lrp6 endocytosis. Proc. Natl. Acad. Sci. U S A. *115*, E9135–E9144. PMID: 30209221. https://doi.org/10.1073/pnas.1812117115.

Dobrowolski, R., Vick, P., Ploper, D., Gumper, I., Snitkin, H., Sabatini, D.D., and De Robertis, E.M. (2012). Presenilin deficiency or lysosomal inhibition enhances Wnt signaling through relocalization of GSK3 to the late-endosomal compartment. Cell Rep. *2*, 1316–1328. PMID: 23122960. https://doi.org/10.1016/j.celrep.2012.09.026.

Doherty, G.J., and McMahon, H.T. (2009). Mechanisms of endocytosis. Annu. Rev. Biochem. *78*, 857–902. PMID: 19317650. https://doi.org/10.1146/annurev.biochem.78.081307.110540.

Du, J., Zu, Y., Li, J., Du, S., Xu, Y., Zhang, L., Jiang, L., Wang, Z., Chien, S., and Yang, C. (2016). Extracellular matrix stiffness dictates Wnt expression through integrin pathway. Scient. Rep. *6*, 20395. PMID: 26854061. https://doi.org/10.1038/srep20395.

Frame, M.C., Fincham, V.J., Carragher, N.O., and Wyke, J.A. (2002). V-Src's hold over actin and cell adhesions. Nat. Rev.Mol. Cell Biol. *3*, 233–245. PMID: 11994743. https://doi.org/10.1038/nrm779.

Gallego-Muñoz, P., Ibares-Frías, L., Garrote, J.A., Valsero-Blanco, M.C., Cantalapiedra-Rodríguez, R., Merayo-Lloves, J., and Carmen Martínez-García, M. (2018). Human corneal fibroblast migration and extracellular matrix synthesis during stromal repair: role played by platelet-derived growth factor-BB, basic fibroblast growth factor, and transforming growth factor-B1. J. Tissue Eng. Regen. Med. *12*, e737–e746. PMID: 27860426. https://doi.org/10.1002/term.2360.

Griffith, E., Coutts, A.S., and Black, D.M. (2005). RNAi knockdown of the focal adhesion protein TES reveals its role in actin stress fibre organisation. Cell Motil. Cytoskelet. *60*, 140–152. PMID: 15662727. https://doi.org/10.1002/cm.20052.

Gu, Z., Noss, E.H., Hsu, V.W., and Brenner, M.B. (2011). Integrins traffic rapidly via circular dorsal ruffles and macropinocytosis during stimulated cell migration. J. Cell Biol. *193*, 61–70. PMID: 21464228. https://doi.org/10.1083/jcb.201007003.

Gruenberg, J., and Stenmark, H. (2004). The biogenesis of multivesicular endosomes. Nat. Rev. Mol. Cell Biol. *5*, 317–323. PMID: 15071556. https://doi.org/10.1038/nrm1360.

Kaplan, K.B., Bibbins, K.B., Swedlow, J.R., Arnaud, M., Morgan, D.O., and Varmus, H.E. (1994). Association of the amino-terminal half of c-Src with focal adhesions alters their properties and is regulated by phosphorylation of tyrosine 527. EMBO J. *13*, 4745–4756, PMID: 7525268.

Kim, N.G., Xu, C., and Gumbiner, B.M. (2009). Identification of targets of the Wnt pathway destruction complex in addition to β-catenin. Proc. Natl. Acad. Sci. U S A. *106*, 5165–5170. PMID: 19289839. https://doi.org/10.1073/pnas.0810185106.

Kim, H., Vick, P., Hedtke, J., Ploper, D., and De Robertis, E.M. (2015). Wnt signaling translocates Lys48-linked polyubiquitinated proteins to the lysosomal pathway. Cell Rep. *11*, 1151–1159. PMID: 26004177. https://doi.org/10.1016/j.celrep.2015.04.048.

Li, H., Huang, K., Gao, L., Wang, L., Niu, Y., Liu, H., Wang, Z., Wang, L., Wang, G., and Wang, J. (2016). TES inhibits colorectal cancer progression through activation of P38. Oncotarget *7*, 45819–45836. PMID: 27323777. https://doi.org/10.18632/oncotarget.9961.

Li, Y., Gonzalez, W.G., Andreev, A., Tang, W., Gandhi, S., Cunha, A., Prober, D., Lois, C., and Bronner, M.E. (2020). Macropinocytosis-mediated membrane recycling drives neural crest migration by delivering F-actin to the lamellipodium. Proc. Natl. Acad. Sci. U S A. *117*, 27400–27411. PMID: 33087579. https://doi.org/10.1073/pnas.2007229117.

Loh, K.M., van Amerongen, R., and Nusse, R. (2016). Generating cellular diversity and spatial form: Wnt signaling and the evolution of multicellular animals. Dev. Cell *38*, 643–655. PMID: 27676437. https://doi.org/10.1016/j.devcel.2016.08.011.

Moreno-Layseca, P., Icha, J., Hamidi, H., and Ivaska, J. (2019). Integrin trafficking in cells and tissues. Nat. Cell Biol. *21*, 122–132. PMID: 30602723. https://doi.org/10.1038/s41556-018-0223-z.

Mylvaganam, S., Freeman, S.A., and Grinstein, S. (2021). The cytoskeleton in phagocytosis and macropinocytosis. Curr. Biol. *31*, R619–R632. PMID: 34033794. https://doi.org/10.1016/j.cub.2021.01.036.

Nieto, M.A., Huang, R.Y., Jackson, R.A., and Thiery, J.P. (2016). EMT: 2016 Cell *166*, 21–45. PMID: 27368099. https://doi.org/10.1016/j.cell.2016.06.028.

Nichols, B.J., and Lippincott-Schwartz, J. (2001). Endocytosis without clathrin coats. Trends Cell Biol. *11*, 406–412. PMID: 11567873. https://doi.org/10.1016/s0962-8924(01)02107-9.

Niehrs, C. (2012). The complex world of Wnt receptor signalling. Nat. Rev. Mol. Cell Biol. *13*, 767–779. PMID: 23151663. https://doi.org/10.1038/nrm3470.

Niehrs, C. (2022). The role of Xenopus developmental biology in unraveling Wnt signalling and antero-posterior axis formation. Dev. Biol. *482*, 1–6. PMID: 34818531. https://doi.org/10.1016/j.ydbio.2021.11.006.

Nieuwkoop, P.D., and Faber, J. (1967). Normal Table of Xenopus laevis (Daudin): A Systematical and Chronological Survey of the Development from the Fertilized Egg till the End of Metamorphosis (North-Holland Publishing Company).

Nusse, R., and Clevers, H. (2017). Wnt/β-catenin signaling, disease, and emerging therapeutic modalities. Cell *169*, 985–999. PMID: 28575679. https://doi.org/10.1016/j.cell.2017.05.016.

Ramirez, C., Hauser, A.D., Vucic, E.A., and Bar-Sagi, D. (2019). Plasma membrane V-ATPase controls oncogenic RAS-induced macropinocytosis. Nature *576*, 477–481. PMID: 31827278. https://doi.org/10.1038/s41586-019-1831-x.

Ramirez, N.E., Zhang, Z., Madamanchi, A., Boyd, K.L., O'Rear, L.D., Nashabi, A., Li, Z., Dupont, W.D., Zijlstra, A., and Zutter, M.M. (2011). The A2β1 Integrin is a metastasis suppressor in mouse models and human cancer. J. Clin. Investig. *121*, 226–237. PMID: 21135504. https://doi.org/10.1172/JCI42328.

Redelman-Sidi, G., Binyamin, A., Gaeta, I., Palm, W., Thompson, C.B., Romesser, P.B., Lowe, S.W., Bagul, M., Doench, J.G., Root, D.E., and Glickman, M.S. (2018). The canonical Wnt pathway drives macropinocytosis in cancer. Cancer Res. *78*, 4658–4670. PMID: 29871936. https://doi.org/10.1158/0008-5472.CAN-17-3199.

Retta, S.F., Balzac, F., Ferraris, P., Belkin, A.M., Fässler, R., Humphries, M.J., De Leo, G., Silengo, L., and Tarone, G. (1998). β-Integrin cytoplasmic subdomains involved in dominant negative

function. Mol. Biol. Cell *9*, 715–731. PMID: 9529373. https://doi.org/10.1091/mbc.9.4.715.

Smith, J.C., and Tata, J.R. (1991). Xenopus cell lines. Methods Cell Biol. *36*, 635–654, PMID: 1811155.

Sun, T., Rodriguez, M., and Kim, L. (2009). Glycogen Synthase Kinase 3 in the world of cell migration. Dev. Growth Differ. *51*, 735–742. PMID: 19891643. https://doi.org/10.1111/j.1440-169X.2009.01141.x.

Swanson, J.A., and King, J.S. (2019). The breadth of macropinocytosis research. Philos. Trans. R. Soc. Lond. B. Biol. Sci. *374*, 20180146. PMID: 30967000. https://doi.org/10.1098/rstb.2018.0146.

Taelman, V.F., Dobrowolski, R., Plouhinec, J.L., Fuentealba, L.C., Vorwald, P.P., Gumper, I., Sabatini, D.D., and De Robertis, E.M. (2010). Wnt signaling requires sequestration of Glycogen Synthase Kinase 3 inside multivesicular endosomes. Cell *143*, 1136–1148. PMID: 21183076. https://doi.org/10.1016/j.cell.2010.11.034.

Tejeda-Muñoz, N., Albrecht, L.V., Bui, M.H., and De Robertis, E.M. (2019). Wnt canonical pathway activates macropinocytosis and lysosomal degradation of extracellular proteins. Proc. Natl. Acad. Sci. U.S.A. *116*, 10402–10411. PMID: 31061124. https://doi.org/10.1073/pnas.1903506116.

Tu, C., Ortega-Cava, C.F., Winograd, P., Stanton, M.J., Reddi, A.L., Dodge, I., Arya, R., Dimri, M., Clubb, R.J., Naramura, M., et al. (2010). Endosomal-sorting complexes required for transport (ESCRT) pathway-dependent endosomal traffic regulates the localization of active Src at focal adhesions. Proc. Natl. Acad. Sci. U S A. *107*, 16107–16112. PMID: 20805499. https://doi.org/10.1073/pnas.1009471107.

Vanlandingham, P.A., and Ceresa, B.P. (2009). Rab7 regulates late endocytic trafficking downstream of multivesicular body biogenesis and cargo sequestration. J. Biol. Chem. *284*, 12110–12124. PMID: 19265192. https://doi.org/10.1074/jbc.M809277200.

Vinyoles, M., Del Valle-Pérez, B., Curto, J., Viñas-Castells, R., Alba-Castellón, L., García de Herreros, A., and Duñach, M. (2014). Multivesicular GSK3 sequestration upon Wnt signaling is controlled by P120-Catenin/Cadherin interaction with LRP5/6. Mol. Cell *53*, 444–457. PMID: 24412065. https://doi.org/10.1016/j.molcel.2013.12.010.

Yokoyama, N., and Malbon, C.C. (2009). Dishevelled-2 docks and activates Src in a Wnt-dependent manner. J. Cell Sci. *122*, 4439–4451. PMID: 19920076. https://doi.org/10.1242/jcs.051847.

Yu, Y., Wu, J., Wang, Y., Zhao, T., Ma, B., Liu, Y., Fang, W., Zhu, W.G., and Zhang, H. (2012). Kindlin 2 forms a transcriptional complex with β-Catenin and TCF4 to enhance Wnt signalling. EMBO Rep. *13*, 750–758. PMID: 22699938. https://doi.org/10.1038/embor.2012.88.

STAR★METHODS

KEY RESOURCES TABLE

REAGENT or RESOURCE	SOURCE	IDENTIFIER
Antibodies		
Zyxin	Abcam	Cat# ab50391; RRID:AB_883768
Vinculin	Abcam	Cat# ab129002; RRID:AB_11144129
p-Src	Cell Signaling	Cat# #2101; RRID:AB_331697
β-catenin	Santa Cruz	Cat# sc-7963; RRID:AB_626807
IRDye 680	Li-Cor	Cat# 926-68072; RRID:AB_10953628
IRDye 800	Li-Cor	Cat# 926-32213; RRID:AB_621848
Donkey anti-rabbit IgG, Alexa Fluor 568 conjugate	Jackson	Cat# 711-166-152; RRID:AB_2313568
Donkey anti-mouse IgG, Alexa Fluor 488 conjugate	Jackson	Cat# 715-546-150; RRID:AB_2340849
GSK3	Abcam	Cat# ab93926, RRID:AB_10563643
ITGβ1	Proteintech	12594-1-AP RRID:AB_2130085
anti-γ-Tubulin	Sigma	Cat# T6557; RRID:AB_477584
Transferrin Receptor (TfR)	ThermoFisher	Cat#13-6800
Chemicals, peptides, and recombinant proteins		
Fibronectin	ThermoFisher	Cat#33016015
Digitonin	Sigma	Cat#300410
Phalloidin	Abcam	Cat#ab176759
Lithium chloride (LiCl)	Sigma	Cat#L4408
Wnt3a	Peprotech	Cat#315-20
10-cm dish	ThermoFisher	Cat#174903
8-well glass-bottom chamber slides	ibidi	Cat#80827
Circular coverslips	ibidi	Cat#10815
12-well dish	ThermoFisher	Cat#150628
DMEM	ThermoFisher	Cat#11965092
L-15	ThermoFisher	Cat#11415064
Glutamine	ThermoFisher	Cat#25030081
Fetal Bovine Serum (FBS)	ThermoFisher	Cat#16000044
Bovine Serum Albumin (BSA)	ThermoFisher	Cat#9048468
Pen-Strep antibiotics	ThermoFisher	Cat#15140122
Triton X-100	ThermoFisher	Cat#HFH10
Paraformaldehyde	Sigma	Cat#P6148
Fibronectin	Sigma	Cat# F4759
PBS	Gibco	Cat#10-010-023
PBS	Fisher Scientific	Cat#BP3994
Lipofectamine 3000	ThermoFisher	Cat#L3000001
Fluoroshield Mounting Medium with DAPI	Abcam	Cat# ab104139
Protease Inhibitors	Roche	Cat#04693132001
Phosphatase inhibitors	Calbiochem	Cat#524629
sulfo-NHS-SS-Biotin	ThermoFisher	Cat#21331
Streptavidin-agarose beads	ThermoFisher	Cat#20353
TNE buffer	Sigma	Cat#T4415
Proteinase K	ThermoFisher	Cat#25530049

(*Continued on next page*)

Continued

REAGENT or RESOURCE	SOURCE	IDENTIFIER
mMESSAGE mMACHINE™ SP6 Transcription Kit	ThermoFisher	Cat#AM1340
RNAeasy Plus kit	QIAGEN	Cat#74034
Roche Sequencing	Roche	Cat# KK8580/ 08098115702
Critical commercial assays		
Dual-Luciferase Reporter Assay System	Promega	Cat#E1500
Deposited data		
GEO, Accession Number GSE193381	NCBI	https://www.ncbi.nlm.nih.gov
Experimental models: Cell lines		
Alexander (hepatocellular carcinoma)	ATCC	RRID:CVCL_0485
HeLa (human cervical adenocarcinoma)	ATCC	RRID: CVCL_0030
SW480	ATCC	RRID:CVCL_0546
Experimental models: Organisms/strains		
Xenopus laevis	Xenopus I	
Oligonucleotides		
Inte-Forward: GGCGGATCCACCATGAATTTACAACCAATTTTCTG	Retta et al., 1998	N/A
Inte-Reverse: GGCATCGAT TATCATTAAAAGCTTCCATATCAG	Retta et al., 1998	N/A
pCS2 Inte-WT- Reverse: GGCATCGATTTTTCCCTCATACTTCGGA	This paper	N/A
5'GTGAATACTGGATAACGGGCCATCT3'	GeneTools	N/A
ITGβ1	Santa Cruz Biotechnology	sc-35674
control siRNAs	Santa Cruz Biotechnology	sc-37007
Recombinant DNA		
LifeAct	IMSR	RRID:IMSR_EM:12427
pCS2-mGFP	Addgene	RRID:Addgene_14757
CD63-RFP	Addgene	RRID:Addgene_62964
xWnt8myc	Addgene	RRID:Addgene_16863
β-catenin Activated Reporter (BAR)	Addgene	RRID:Addgene_12456
Renilla reporter	Addgene	RRID:Addgene_62186
Software and algorithms		
ImageJ	NIH	http://imagej.nih.gov/ij/
Axiovision 4.8	Zeiss	http://Zeiss.com
Zen 2.3 imaging software	Zeiss	http://Zeiss.com
R	R Core Team	https://cran.r-project.org
2200 TapeStation	Agilent Technologies	https://www.agilent.com
Fastp	Chen et al., 2018	N/A
Other		
IM 300 microinjection pump	Narishige International USA, Inc	N/A
Axio Observer Z1 Inverted Microscope with Apotome	Zeiss	N/A

RESOURCE AVAILABILITY

Lead contact

Further information and requests for resources and reagents should be directed to and will be fulfilled by the Lead Contact, Dr. Edward M. De Robertis (ederobertis@mednet.ucla.edu).

Materials availability

No custom code, software, or algorithm central to supporting the main claims of the paper were generated in this manuscript.

Data and code availability

The complete RNAseq data reported in this paper have been deposited in GEO, Database: GSE193381. This paper does not report original code.

EXPERIMENTAL MODEL AND SUBJECT DETAILS

Tissue culture and transfection

HeLa (ATCC, CRL-2648), HEK-293BR (BAR/Renilla), NIH 3T3, Alexander cells (RRID:CVCL_0485), and HCSF cells were cultured in DMEM (Dulbecco's Modified Eagle Medium), supplemented with 10% fetal bovine serum, 1% glutamine, and penicillin/streptomycin. Cells were cultured at 37°C in 5% CO_2 atmosphere. The cells were seeded to maintain a cell density between 20 and 60% and experiments were performed when cells reached a confluence of 70–80%. Cells were transfected by Lipofectamine 3000. DNA constructs were added to cells and incubated overnight, with a fresh change of media after 12-16 h. Cells were transferred to 2% of fetal bovine serum 6-12 h after transfection before treatment with Wnt3a (Preprotech Cat# 315-20) protein at 100 ng/mL.

Xenopus embryo microinjection

Xenopus laevis embryos were fertilized *in vitro* using excised testis. Staging was as described (Nieuwkoop and Faber, 1967). *In vitro* synthesized mRNAs were introduced into embryos by microinjection using an IM 300 Microinjector (Narishige International USA, Inc) 4 times. pCS2-hITGβ1, was linearized with NotI and transcribed with SP6 RNA polymerase using the Ambion mMessage mMachine kit. Embryos were injected in 1x MMR and cultured in 0.1x MMR (Albrecht et al., 2020). To study the role of ITGβ1 in the Wnt pathway, we designed an ITGβ1 antisense MO against *Xenopus* ITGβ1. Injection of 4 nl of 0.3 mM MO four times into the animal pole of 4-cell stage embryos was without phenotypic effect. However, ITGβ1 MO interfered with the dorsalization caused by the radial injection of *Wnt8myc* mRNA (0.5 pg) (Ding et al., 2018). This effect was specific to ITGβ1 as axial development could be rescued by co-injection of 100 pg of human *ITGβ1* mRNA.

Animal cap cell culture

Animal caps were dissected at early blastula stage 8.5 to 9 in 1 x MMR solution, washed 3 times, and cells cultured in L-15 medium containing 10% Fetal Calf Serum diluted to 50% with H_20 (Smith and Tata 1991) on fibronectin-coated coverslips for 12-18 h. When mounting with coverslips, a drop of Anti-fade Fluorescence Mounting Medium-Aqueous, Fluoroshield was added and microscopic examination of RFP and GFP was performed. Image acquisition was performed using a Carl Zeiss Axio Observer Z1 Inverted Microscope with Apotome.

Antibodies and reagents

Antibodies against the focal adhesion protein Zyxin (ab50391, 1:200), Vinculin (ab129002, 1:200), Phalloidin (ab176759, 1:1000), and the serine-threonine kinase GSK3 (ab93926, 1:4000) were obtained from Abcam. ITGβ1 antibody was obtained from Proteintech (12594-1-AP, 1:100), while anti-γ-Tubulin antibody was obtained from Sigma (T6557, 1:3000). Secondary antibodies for immunostaining (1:500) were from Jackson ImmunoResearch Laboratories, Inc (715166150, 711545152). Secondary antibodies coupled to Infrared Dyes (IRDye 680 (926–68072) and IRDye 800 (926–32213) at 1:3000 (LI-COR) were used for western blots and analyzed with the LI-COR Odyssey system.

Primers for cloning human DN-ITGβ1 into pCS2 c-terFlag were Inte-Forward: GGCGGATCCACCATGAA TTTACAACCAATTTTCTG, Inte-Reverse: GGCATCGAT TATCATTAAAAGCTTCCATATCAG. Primers for cloning human ITGβ1-WT into pCS2 Inte-WT- Reverse: GGCATCGATTTTTCCCTCATACTTCGGA. Pools of 3 target-specific ITGβ1 (sc-35674) and control siRNAs (sc-37007) were obtained from Santa Cruz Biotechnology. *Xenopus laevis* ITGβ1 antisense MO, sequence 5'GTGAATACTGGATAACGGGCCATCT3', was designed with the help of GeneTools.

METHOD DETAILS

Immunostainings

HeLa or HCSF cells were plated on glass coverslips and then directly transfected, or alternatively transfected with a later split onto coverslips. Coverslips were acid-washed and treated with fibronectin

(10 μg/ml for 30 min at 37°C, Sigma F4759) to enhance cell spreading and adhesion. Cells were fixed with 4% paraformaldehyde (Sigma #P6148) 15 min, permeabilized with 0.2% Triton X-100 in phosphate-buffered saline (PBS; Gibco) for 10 min, blocked with 5% BSA in PBS for 1 hour. Primary antibodies were added overnight at 4°C. The samples were washed three times with PBS, and secondary antibodies were applied for one hour at room temperature. After three additional washes with PBS, the coverslips were mounted with Fluoroshield Mounting Medium with DAPI (ab104139). Immunofluorescence was analyzed and photographed using a Zeiss Imager Z.1 microscope with Apotome.

Western blots

Cell lysates were prepared using RIPA buffer (0.1% NP40, 20 mM Tris/HCl pH 7.5), 10% Glycerol, together with protease (Roche #04693132001) and phosphatase inhibitors (Calbiochem #524629).

Cell Surface Biotin Labeling

HeLa cells were incubated with Wnt3a for 0, 15, and 30 min at 37°C. The cells were placed on ice and washed three times with ice-cold PBS (Fisher Scientific), and then labeled with non-cell permeable sulfo-NHS-SS-Biotin (1 mg/ml) for 30 min using rotary agitation at 4°C (Ding et al., 2018). The cells were washed three times with ice-cold quenching solution (50 mM Glycine in PBS, pH 7.4), and with ice-cold PBS. Cell lysates were prepared using a RIPA buffer and incubated with Streptavidin-agarose beads (Thermo Scientific) using end-over-end agitation at 4°C overnight. An aliquot of the original cell lysate was saved for input control. The resin was washed 3 x with TNE buffer (Sigma) and then an equal volume of 2 x SDS loading sample buffer was added, and heated at 95°C for 5 min. The samples were electrophoresed by polyacrylamide gel electrophoresis (PAGE), and transferred to a nitrocellulose membrane using a semi-dry transfer apparatus (1 hour at 15 V). The membranes were blocked (TBS with skimmed milk 5%) for an hour. Later the membrane was incubated with primary (overnight) and secondary antibodies (60 minutes), and blots were developed using the LiCor Odyssey system.

Protease protection assay

Cells were plated on glass coverslips and after 24 h were treated with or without Wnt3a for 20 min. They were placed on ice, permeabilized with digitonin (6.5 μg/mL) for 30 min, and incubated with Proteinase K (1 μg/mL) for 10 min (Albrecht et al., 2018). As a control, the addition of Triton X-100 (0.01%) was used to dissolve all cell membranes. Samples were then analyzed by immunofluorescence.

Luciferase assay in animal caps

For measurement of beta-catenin activation reporter (BAR) in ectodermal explant experiments, *Xenopus* embryos were injected four times into the animal pole at the 4-cell stage with *xWntmyc* (0.5 pg) mRNA together with reporter plasmids for (BAR-Luciferase 50 pg and CMV-Renilla, 5 pg), and with synthetic *WT-* or *DN-hITGβ1* mRNAs (400 pg). Animal caps were dissected at stage 9.5 and Luciferase activity was measured with the Dual-Luciferase Reporter Assay System (Promega) according to manufacturer's instructions, using the Glomax Luminometer (Promega). Luciferase values of each sample were normalized for Renilla activity.

Library preparation and illumina sequencing

RNA was isolated with the RNAeasy Plus kit (QIAGEN) from 500 to 900 × 10^3 cells. Four independent cultures of matched HCC ± Axin1 cells were used. The quality and concentration of the extracted material were assessed using the RNA assay on a 2200 TapeStation (Agilent Technologies): all the samples had a RIN score higher than 8. Libraries were constructed with the KAPA mRNA Hyper-Prep kit (Roche Sequencing, cat# KK8580/08098115702) with unique dual-indexed adapters according to the manufacturer''s protocol. Final library QC qPCR quantitation was performed using the D1000 assay on a 2200 TapeStation (Agilent Technologies). After concentration normalization, libraries were pooled and sequenced on a NovaSeq 6000 (Illumina) SP lane (2 × 150).

Sequencing data processing

After sequencing, demultiplexed reads (Illumina bcl2fastq) were processed to remove the adapters using fastp (Chen et al., 2018). Trimmed reads were aligned against the GRCh38 genome using STAR (v2.7.4.a). The counts assigned to each gene were combined into a matrix and subject to differential expression

analysis using DESeq2. The complete RNAseq data reported in this paper have been deposited in GEO, Accession Number GSE193381.

Heatmap

Normalized raw counts (DESeq2) were used as input for unbiased heatmap visualization using the R package heatmap with the following options: scale = 'row', cutree_rows = 4, cluster_cols = TRUE, cluster_rows = TRUE. Only genes defined as members of the Integrin pathway (BioCarta) are shown.

QUANTIFICATION AND STATISTICAL ANALYSIS

Image quantification

The data are expressed as means and standard errors of the mean (SEM). Statistical analysis of the data was performed using the Student t-test. A p value of <0.01 was considered statistically significant. The number of vesicles in the immunofluorescence was quantified from the DIC light microscope channel using the ImageJ software and a computer-assisted particle analysis tool. Individual channels were given thresholds with MaxEntropy. The individual vesicles were separated using the "binary watershed" function and vesicles were counted using the "analyze particles" function, with particle size 0.2–5 μm and circularity –1. More than 25 cells were counted per experiment. They were numbered, outlined, and then copied to a spreadsheet in order to perform the statistical analysis. To quantify colocalization of molecules in vesicles, Pearson's correlation coefficients were calculated using ImageJ software to assess the degree of colocalization comparing two different channels using $n > 25$ cells per condition.